Electroluminescent Properties of Spiro[fluorene-benzofluorene]-Containing Blue Light Emitting Materials

Soon-Ok Jeon, Hyun-Seok Lee, Young-Min Jeon, Joon-Woo Kim,† Chil-Won Lee,† and Myoung-Seon Gong*

Department of Chemistry and Institute of Basic Science, Dankook University, Chungnam 330-714, Korea
**E-mail: msgong@dankook.ac.kr*
†*OLED Team, Daejoo Electronic Materials, Siheung, Kyunggi 429-848, Korea*
Received October 28, 2008, Accepted February 23, 2009

New spiro[fluorene-7,9′-benzofluorene]-based blue host material, 5-phenyl-spiro[fluorene-7,9′-benzofluorene] (BH-1P), was successfully prepared by reacting 5-bromo-spiro[fluorene-7,9′-benzofluorene] (**1**) with phenyl boronic acid through the Suzuki reaction. 5-(*N*,*N*-Diphenyl)amino-spiro[fluorene-7,9′-benzofluorene] (BH-1DPA) and diphenyl-[4-(2-[1,1;4,1]terphenyl-4-yl-vinyl)-phenyl]amine (BD-1) were used as dopant materials. 2,5-Bis-(2′,2″-bipyridin-6-yl)-1,1-diphenyl-3,4-diphenylsilacyclopentadiene (ET4) and Alq_3 were used as electron transfer materials. Their UV absorption, photoluminescence and thermal properties were examined. The blue OLEDs with the configuration of ITO/DNTPD/α-NPD/BH-1P:5% dopant/Alq_3 or ET4/LiF-Al prepared from the BH-1P host and BH-1DPA and BD-1 dopants showed a blue EL spectrum at 452 nm at 10 V and a luminance of 923.9 cd/m^2 with an efficiency of 1.27 lm/W at a current density of 72.57 mA/cm^2.

Key Words: Blue OLED, Host, Dopant, Spiro[fluorene-benzofluorene], Color purity

Introduction

Since Tang and Vanslyke[1] first reported the fabrication of organic light emitting diodes (OLEDs) with high efficiency in 1987, OLEDs have been intensively investigated for their potential applications in the fields of flat-panel displays. However, achieving a full color display still remains a significant challenge, because the luminescence efficiency of blue OLEDs is still very low and, furthermore, obtaining pure emission colors from organic molecules is difficult.[2,3] In order to eliminate these obstacles, many methods have been adopted, including the use of an emitting-assist dopant,[4] the introduction of a new device structure[5] and the development of an original host material[6] to improve the energy transfer from host to guest.

Since Tour *et al.* introduced the spirobifluorene unit into organic electronics in 1996,[7] spirobifluorene containing oligomers and polymers have become promising candidates for electroluminescent materials, due to their high luminescence efficiency, carrier mobility, and excellent thermal stability. Salbeck *et al.* exploited spirobifluorene building blocks to construct various oligomers.[8] Fully spiro-configured terfluorenes and spirobifluorene-linked anthracene derivatives have also been synthesized and used as blue light-emitting materials with high thermal stability.[9] Carriertransporting materials of spirobifluorene with a high glass transition temperature also show excellent nondispersive hole transporting and ambipolar carrier transporting properties.[10]

Incorporation of various aromatic substituents to the spirobifluorene is an useful strategy to expand the application of spiro compounds. However, spiro compounds with versatile substituents, especially spiro[fuorene-benzofluorene] with an asymmetric substitution pattern on the fluorine and benzofluorene units, have seldom been reported.[11-16] Recently, we have successfully demonstrated that the spiro[fluorene-7,9′-benzofluorene]-based host and dopant materials can form a blue OLED with a good color purity.[17-22]

In this study, new host materials based on the new spiro-[fluorene-7,9′-benzofluorene]-based materials, BH-1P and BH-1DPA, were designed and synthesized by the Suzuki reaction and amination reaction in order to improve the EL efficiency and color purity of the OLEDs. We report the investigation of the blue OLEDs derived from these new blue spiro-type host material.

Experimentals

Materials and Measurements. Tetrakis(triphenylphosphine)-palladium(0), phenyl boronic acid and potassium *t*-butoxide (Aldrich Chem. Co.) were used without further purification. Phenyl boronic acid (Frontier Scientific CO.) were used without further purification. Tetrahydrofuran and toluene were distilled over sodium and calcium hydride. 5-Diphenyl amino-spiro[fluorene-7,9′-benzofluorene] (BH-1DPA) and 5-bromo-spiro[fluorene-7,9′-benzofluorene] (**1**) were prepared by the method previously reported.[17] Diphenyl[4-(2-[1,1;4,1]terphenyl-4-yl-vinyl)-phenyl]-amine (BD-1) and 2,5-bis-(2′,2″-bipyridin-6-yl)-1,1-diphenyl-3,4-diphenylsilacyclopentadiene (ET4) were used as a dopant and electron transfer material, respectively.

The FT-IR spectra were obtained with a Biorad Excaliber FTS-3000MX spectrophotometer and the ^{1}H NMR and ^{13}C NMR spectra were recorded on a Bruker Avance 500 (500 MHz) spectrometer. The photoluminescence (PL) spectra were recorded on a fluorescence spectrophotometer (Jasco FP6500) and the UV-vis spectra were obtained by means of a UV-vis spectrophotometer (Shimadzu, UV-1601PC). The elemental analyses were performed using a CE Instrument EA1110. The DSC measurements were performed on a Mettler DSC 822e under nitrogen at a heating rate of 10

°C/min. The low and high resolution mass spectra were recorded using a JEOL JMS-AX505WA spectrometer in FAB mode. The energy levels were measured with a low energy photo electron spectrometer (Riken-Keiki AC-2).

Synthesis of 5-phenyl-spiro[fluorene-7,9′-benzofluorene] (BH-1P). 5-Bromo-spiro[fluorene-7,9′-benzofluorene] (**1**) (10.0 g, 22.4 mmol), phenyl boronic acid (3.17 g, 26.1 mmol) and tetrakis(triphenylphosphine)palladium(0) (1.29 g, 1.12 mmol) dissolved in THF (100 mL) were stirred in a two-necked flask under a nitrogen atmosphere for 1 h. To the above reaction mixture was added a solution of potassium carbonate (2 M, 100 mL) dissolved in distilled water (50 mL) dropwise over a period of 30 min. The reaction mixture was refluxed for 12 h at 90 °C under a nitrogen atmosphere. After being cooled to ambient temperature, the reaction mixture was extracted with dichloromethane and water. The organic layer was evaporated with a rotary evaporator. The residue was subjected to column chromatography (silica gel) using *n*-hexane and a white powdery product was obtained.

Yield 68%. Mp: 259 °C. ^{1}H NMR (500 MHz, $CDCl_3$) δ 8.94-8.92 (d, 1H), 8.47-8.45 (d, 1H), 7.99-7.97 (d, 1H), 7.84-7.82 (d, 1H), 7.73-7.70 (t, 2H), 7.50-7.45 (q, 3H), 7.35-7.30 (m, 7H), 7.15-7.12 (t, 2H), 7.10-7.07 (t, 2H), 6.81-6.79 (d, 1H), 6.76-6.75 (d, 1H). ^{13}C NMR ($CDCl_3$): δ 149.9, 148.1, 142.3, 141.1, 140.9, 132.4, 130.3, 128.2, 128.0, 127.7, 127.4, 127.1, 126.8, 125.7, 124.3, 124.2, 123.2, 120.2, 77.4, 77.2, 76.9, 66.5 FT-IR (KBr, cm^{-1}) 3059, 3040, 3012 (aromatic C-H). MS (FAB) m/z 442.0 [(M+1)$^+$]. Anal. Calcd. for $C_{39}H_{24}$ (442.55) $C_{35}H_{22}$: C, 94.99; H, 5.01. Found: C, 94.55; H, 4.96. UV-vis (THF): λ_{max} (Absorption) 343, 325, 302 nm, λ_{max} (Emission) 420, 423 nm.

OLED fabrication and measurement. Prior to device fabrication, ITO with a resistance of 12 Ω/□ on glass was patterned as an active area of 4 mm^2 (2 mm x 2 mm). The substrates were cleaned by sonication in deionized water, boiled in IPA for 20 min, and dried with nitrogen. Finally, the substrates were dry cleaned using plasma treatment in an O_2 and Ar environment. Organic layers were deposited sequentially by thermal evaporation from resistively heated alumina crucibles onto the substrate at a rate of 1.0 Å/s. The thicknesses of the *N,N′*-bis-[4-(di-*m*-tolylamino)phenyl]-*N,N′*-diphenylbiphenyl-4,4′-diamine (DNTPD, HIL), bis[*N*-(1-naphthyl)-*N*-phenyl]benzidine (α-NPD, HTL), host: 5% dopant (EML) and aluminum tris(8-hydroxyquinoline) (Alq_3, ETL) layers were about 400, 200, 300 and 200 Å, respectively. Before the deposition of the metal cathode, LiF was deposited onto the organic layers with a thickness of 10 Å. A high-purity aluminum cathode was deposited at a rate of 1-5 Å/s with a thickness of 2000 Å as the top layer. After the fabrication of the device, the evaporation chamber was vented with nitrogen gas and the device immediately transferred to a glove box. A thin epoxy adhesive was applied from a syringe around the edge of a clean cover glass. To complete the package, a clean cover glass was placed on the top of the device. The epoxy resin was cured under intense UV radiation for 3 min. The current-voltage characteristics of the encapsulated devices were measured on a programmable electrometer having current and voltage sources (Keithley model 237 Source Measure Unit). The luminance and EL spectra were measured with a PR650 system (Photo Research Co. Ltd.).

Results and Discussion

Synthesis and characterization. 5-Phenyl-spiro[fluorene-7,9′-benzofluorene] (BH-1P) was prepared by the Suzuki reaction of **1** with phenyl boronic acid as illustrated in Schemes 1. BH-1P was identified and characterized by FT-IR, ^{1}H NMR and ^{13}C NMR spectroscopy. The results of the elemental analysis and mass spectroscopy also supported the formation of BH-1P and matched well with the calculated data. The spiro-type dopant material, 5-diphenyl amino-spiro-[fluorene-7,9′-benzofluorene] (BH-1DPA), was synthesized by the amination reaction of **1** with diphenylamine according to the method previously reported in the literature.[17]

Optical properties. Figure 1 shows the absorption and photoluminescence spectra of BH-1P, BH-1DPA and BD-1 in

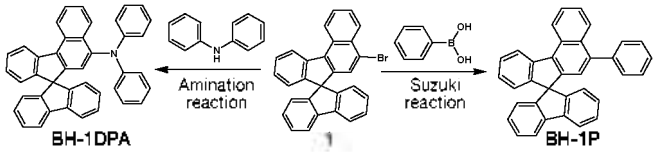

Scheme 1. Synthetic scheme of host and dopant.

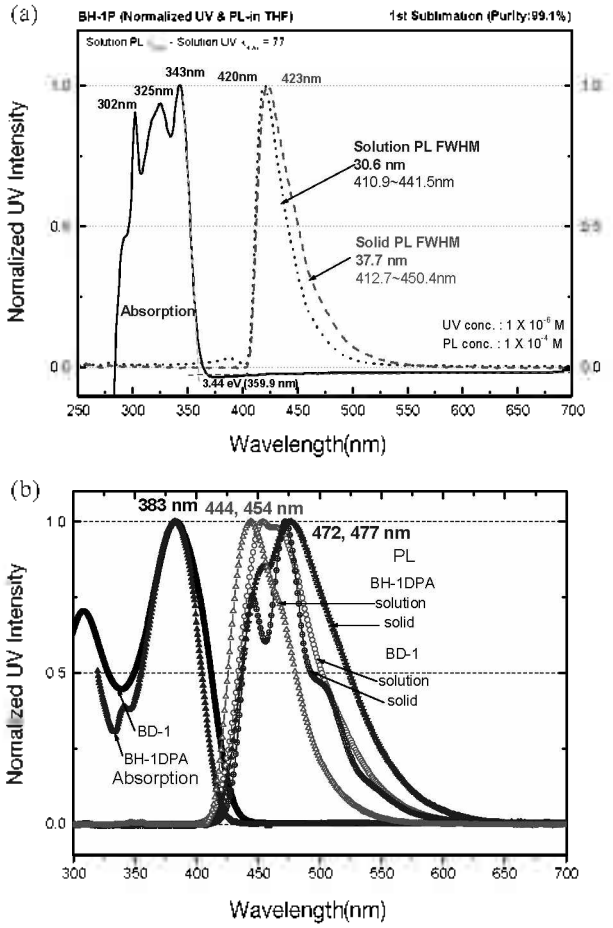

Figure 1. Normalized absorption and photoluminescence spectra of (a) BH-1P host and (b) BD-1 and BH-1DPA dopant materials.

Table 1. The various properties of BH-1P, BH-1DPA and BD-1

Properties	Instrument	Units	BH-1P	BH-1DPA	BD-1
Purity	HPLC	%	99.11	99.5	99
Thermal analysis	DSC	T_g[a] (°C)	115	110.4	-
		T_m[b] (°C)	259	-	306.1
Optical analysis	UV	λ_{max} (nm)	343	383	383
		B_g[c] (eV)	3.44	2.96	2.87
	PL	λ_{max} (nm)	420	444	454
		FWHM[d] (nm)	30.6	38.1	68.5
	Solid PL	Max (nm)	423	477	472
		FWHM[d] (nm)	37.7	87	54
Electrical analysis	AC-2	HOMO[e] (eV)	5.97	5.66	5.46
		LUMO[f] (eV)	2.53	2.70	2.57

[a]Melting temperature. [b]Glass transition temperature. [c]Band gap. [d]Full width at half maximum. [e]Highest occupied molecular orbital. [f]Lowest unoccupied molecular orbital.

Table 2. Electroluminescent properties of devices derived from BH-1P Host materials at 7 and 10 V

Properties \ Devices[a]		1	2	3	4	5	6
EL at 7 V	λ_{max} (nm)	452	448	444	448	444	440
	mA/cm^2	5.55	4.56	3.77	5.14	2.81	4.01
	cd/A	0.95	0.85	1.80	1.59	0.82	0.72
	lm/W	0.42	0.38	0.81	0.71	0.36	0.32
	cd/m^2	52.82	38.91	68.13	82.23	2.18	29.24
	CIE-x	0.16	0.15	0.14	0.15	0.15	0.15
	CIE-y	0.11	0.11	0.10	0.09	0.07	0.07
EL at 10 V	mA/cm^2	84.53	62.95	40.23	72.57	42.48	59.59
	cd/A	0.89	0.62	1.31	1.27	0.65	0.68
	lm/W	0.28	0.20	0.41	0.40	0.20	0.22
	cd/m^2	753.8	391.0	528.0	923.9	276.3	400.6
	CIE-x	0.15	0.15	0.15	0.15	0.15	0.15
	CIE-y	0.09	0.10	0.09	0.09	0.07	0.07

[a]1. BH-1P:5% BH-1DPA/ET4, 2. BH-1P:5% BH-1DPA/Alq_3, 3. BH-1P:5% BD-1/ET4, 4. BH-1P:5% BD-1/Alq_3, 5.BH-1P/ET4, 6. BH-1P/Alq_3

THF solution and in the solid state. In the UV-vis spectra, the maximum absorption wavelengths of BH-1P, BH-1DPA and BD-1 appeared at λ_{max} = 343, 383 and 383 nm, respectively. Upon UV excitation with their maximum wavelengths, the three solutions showed a blue PL with emission maxima at 420, 444 and 454 nm, respectively. This observation suggests that the chiral carbon atom at the spiro[fluorene-7,9′-benzofluorene] center serves as a conjugation interrupt, with the effect of retaining the desired optical properties of the spiro-moiety. The emission spectra of the BH-1P and BH-1DPA thin films, prepared by spin-coating from a toluene solution onto a quartz plate, are similar to those in dilute solution and exhibit red-shifts of 3 and 33 nm, respectively, as shown in Figure 1(a) and Figure 1(b). The various optical properties of BH-1P, BH-1DPA and BD-1 are summarized in Table 1.

Thermal properties. The thermal properties of BH-1P and BH-1DPA were investigated by differential scanning calorimetry (DSC). DSC was performed in the temperature range from 25 to 400 °C. When BH-1P was heated for the first heating cycle, an endothermic peak corresponding to the melting transition was observed at 259 °C , as shown in Figure 2. When the amorphous glass was heated for the second cycle, a second-order transition phenomenon was observed at 115 °C, which is defined as the glass transition temperature (T_g) of BH-1P. The DSC measurements of BH-1DPA showed that upon first heating, it revealed a glass transition temperature (T_g) at 112 °C on heating and melted at 265 °C. On the second heating, no melting points were observed, even though it was given enough time to cool in air. These results imply that BH-1DPA forms an amorphous yellow solid directly after the first heating. Once it becomes an amorphous solid, it does not revert to the crystalline state at all. As a result, the amorphous glassy state of the transparent film of BH-1DPA is a good candidate as an EL material.

Energy levels of materials. The highest-occupied molecular orbital (HOMO) and the corresponding lowest-unoccupied molecular orbital (LUMO) levels were determined from the

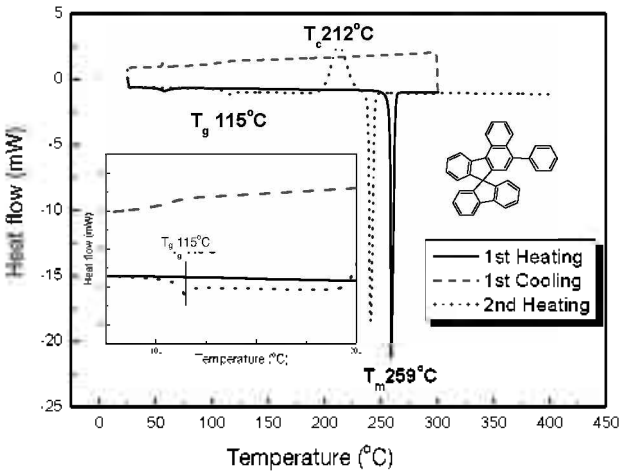

Figure 2. DSC thermograms of BH-1P on heating 10 °C/min and cooling in air.

absorption edge of the optical absorption spectrum of the BH-1P film on a quartz substrate. The energy gap was calculated to be *ca.* 3.44 eV from the UV-vis absorption. The HOMO energy level of BH-1P was determined to be 5.97 eV and the LUMO level was calculated to be 2.53 eV by subtracting the HOMO/LUMO band gap from the HOMO level. The energy level diagram of the blue BH-1P is shown in Figure 3.

EL properties. To study the EL properties of BH-1P, multilayer devices with the configuration of glass ITO anode/hole injection layer (HIL)/hole transport layer (HTL)/emitting layer (EML)/electron transport layer (ETL)/electron injection layer (EIL)/Al cathode were fabricated. 4,4′-Bis[*N*-[4-(*N*,*N*-di-*m*-tolylamino)phenyl]-*N*-phenylamino]biphenyl(DNTPD) was used as the HIL, bis[*N*-(1-naphthyl)-*N*-phenyl]benzidine (α-NPD) as the HTL, BH-1P:5% dopant as the EML and

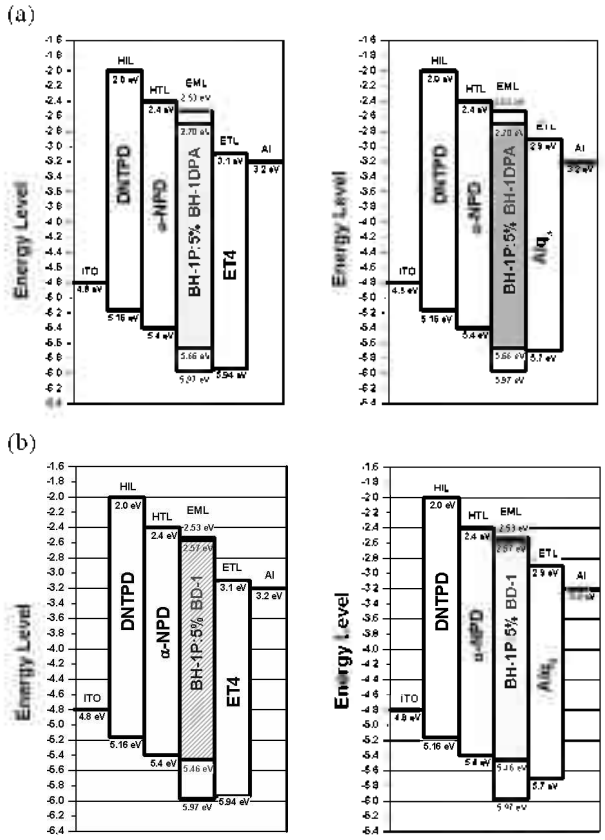

Figure 3. Energy diagrams of BH-1P doped with (a) BH-1DPA (b) BD-1.

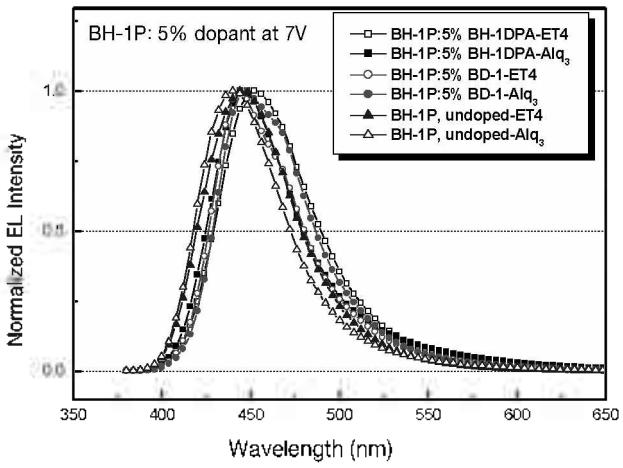

Figure 4. EL spectra of the devices obtained from BH-1P host doped with various dopant materials.

2,5-bis-(2',2"-bipyridin-6-yl)-1,1-diphenyl-3,4-diphenylsilacyclopentadiene (ET4) or tris(8-quinolinolato) aluminum (Alq_3) as the ETL; LiF was used as the EIL.

In the EL spectra of the devices, the peak wavelength is stabilized at around 440-452 nm at 7 V, as shown in Figure 4. It can be seen that the devices doped with BD-1 and BH-1DPA emit blue light having a maximum wavelength at around 448-452 nm and the full width at half maximum

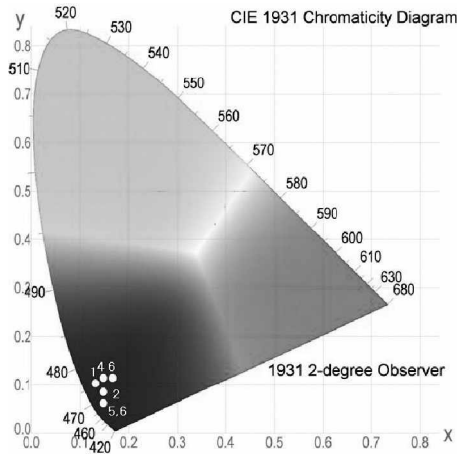

Figure 5. The CIE 1931 coordinates diagram of device (1) BH-1P:5% BH-1DPA/ET4 (0.14, 0.10), (2) BH-1P:5% BH-1DPA/Alq_3 (0.15, 0.09), (3) BH-1P:5% BD-1/ET4 (0.16, 0.11), (4) BH-1P:5% BD-1/Alq_3 (0.15, 0.11), (5) BH-1P/ET4 (0.15, 0.07) and (6) BH-1P/Alq_3 (0.15, 0.07).

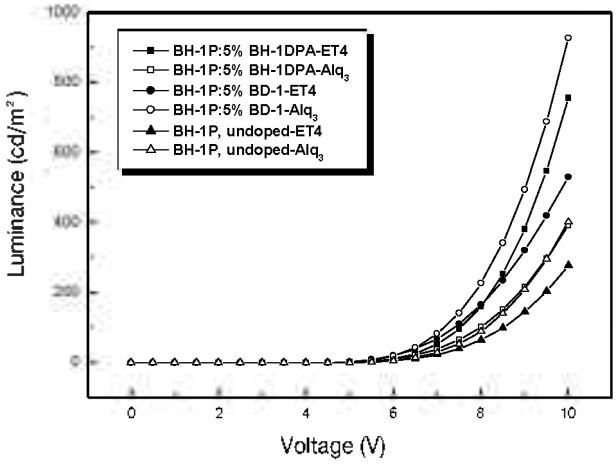

Figure 6. Luminance-voltage curves for the devices using BH-1P host material.

(FWHM) is about 56-60 nm. The EL peak is observed at 440 nm for the device without a dopant, while it was shifted by 12 nm to a longer wavelength in the case of the device made using BH-1P doped with BH-1DPA, with CIE coordinates between (x = 0.16, y = 0.11) and (x = 0.15, y = 0.09). When BD-1 was used as the dopant material, the emitted light had a good color purity with CIE coordinates of (x = 0.15, y = 0.09), as shown in Figure 5.

Device properties. Figure 6 shows the luminance-voltage characteristics of the BH-1P doped with BH-1DPA and BD-1. The initial light output of the device made from BH-1P:5% dopant occurs at 4.5 V. There was a large difference between the luminance of BH-1P:BD-1/ET4 and BH-1P:BD-1/Alq_3 having ET4 and Alq_3 as the electron transport material, with luminances of 528.0 and 923.9 cd/m^2 being obtained at 10 V, respectively.

Figure 7 illustrates the luminance efficiency-voltage characteristics of the devices. Comparing the device consisting of

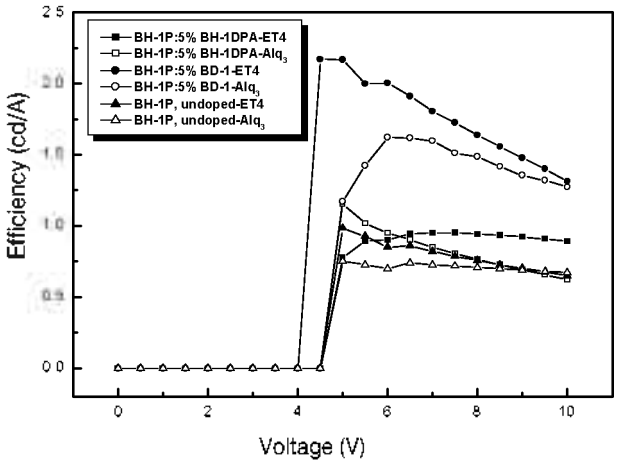

Figure 7. Efficiency-voltage characteristics of the devices using BH-1P host material.

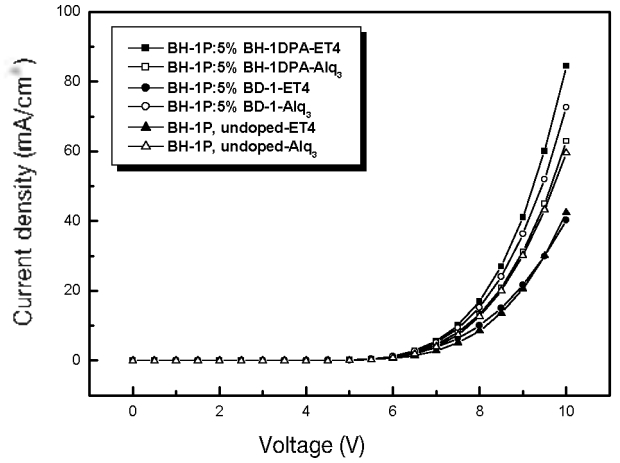

Figure 8. Current density-voltage characteristics of the devices using BH-1P host material.

BH-1P:5% BD-1 with that consisting of BH-1P:5% BH-1DPA, the BD-1 dopant improved the luminance efficiency and color purity to a greater extent. In the device with the structure, BH-1P:5% BD-1/Alq_3, the amount of energy transfer was limited. There was a small difference between the band gaps of the HOMO for the BH-1DPA and BD-1 dopants. BD-1 was slightly influenced by the host material and the efficiency of this material is better than that of BH-1DPA. The luminance efficiency using Alq_3 is better than that of ET4, because of the ease of electron transfer originating from its small energy barrier, according to the schematic energy diagrams.

Figure 8 shows the current density-voltage characteristics for the devices. The turn-on voltage of the devices using BH-1P:5% BD-1/Alq_3 and BH-1P:5% BH-1DPA/ET4 is 4.5 V. The maximum luminance of the above two devices are 923.9 and 753.8 cd/m^2 at current densities of 72.57 and 84.53 mA/cm^2 at 10 V, respectively. The performance of the devices may be further improved with the optimization of the device structure or the control of the BH-1DPA layer using the dopant material. Both the color purity (x = 0.15, y = 0.09) and

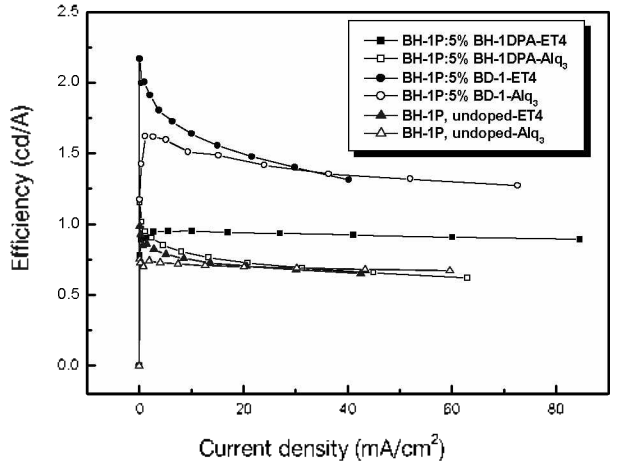

Figure 9. Efficiency-current density characteristics of the device using BH-1P host material.

current efficiency (1.27 cd/A) of the device using BD-1 are better than those of the one using BH-1DPA (391 cd/m^2, 0.62 cd/A and (x = 0.15, y = 0.10)) in the same device structure. When the BH-1DPA and BD-1 films were coated on quartz glass by thermal evaporation with the same thickness, the PL efficiency of the BH-1DPA film, which was examined at the excitation wavelength of their maximum absorption point, was higher than that of BD-1. This result indicates that the device using BH-1DPA has a higher current density than the one using BD-1.

Figure 9 shows that efficiency-current density characteristic of the devices. Both electron transfer and injection occurred between the host and dopant materials, resulting in an improvement of the efficiency. The device made using BH-1P:5% BD-1/ET4 showed an efficiency of 2.17 cd/A at 4.5 V, which was twice as high as that of the device made using BH-1P:5% BH-1DPA/ET4. Based on these results, it was found that the spiro-type host and BD-1 dopant materials are very effective in improving the EL efficiency.

Conclusion

We report the fabrication of blue OLEDs using the new spiro[fluorene-7,9′-benzofluorene]-type host material, BH-1P, doped with BH-1DPA and BD-1 as an emissive dopant in an electron-transporting Alq_3 or ET4 layer. The device doped with BD-1 shows the highest luminance and efficiency resulting from the exciplex emission, with pure blue emission CIE chromaticity coordinates (x = 0.15, y = 0.09). This device can achieve a luminance of 923.9 cd/m^2 with an efficiency of 0.4 lm/W at a current density of 72.57 mA/cm^2. The measurement tests of the lifetime for the devices and the EL characteristics of the devices made with BH-1P using other commercially available dopants are now in progress. These results will be presented elsewhere in the near future.

Acknowledgments. This work was supported by grant No. RT104-01-02 from the Regional Technology Innovation program of the Ministry of Knowledge Economy.

References

1. Tang, C. W.; VanSlyke, S. A. *Appl. Phys. Lett.* **1987**, *51*, 913.
2. Campos, R. A.; Kovalev, I. P.; Guo, Y.; Wakili, N.; Skotheim, I. *J. Appl. Phys.* **1996**, *80*, 7144.
3. Bradley, D. D. C.; Weaver, M. S.; Lidzey, D. G.; Fisher, T. A. *Thin Solid Films* **1996**, *273*, 39.
4. Hamada, Y.; Kanno, H.; Tsujioka, T.; Takahashi, H.; Usuki, T. *Appl. Phys. Lett.* **1999**, *75*, 1682.
5. Xie, Z. Y.; Hung, L. S.; Lee, S. T. *Appl. Phys. Lett.* **2001**, *79*, 1048.
6. Juan, Q.; Yong, Q.; Liduo, W. *Appl. Phys. Lett.* **2002**, *81*, 4913.
7. Wu, R.; Schumm, J. S.; Pearson, D. L.; Tour, J. M. *J. Org. Chem.* **1996**, *61*, 6906.
8. Salbeck, J.; Yu, N.; Bauer, J.; Weissortel, F.; Bestgen, H. *Synth. Met.* **1997**, *91*, 209.
9. Katsis, D.; Geng, Y. H.; Ou, J. J.; Culligan, S. W.; Trajkovska, A.; Chen, S. H.; Rothberg, L. J. *Chem. Mater.* **2002**, *14*, 1332.
10. Bach, U.; Cloedt, K. D.; Spreitzer, H.; Gratzel, M. *Adv. Mater.* **2000**, *12*, 1060.
11. Mitschke, U.; Bäuerle, P. *J. Chem. Soc.* **2001**, 740.
12. Saragi, T. P. I.; Spehr, T.; Siebert, A.; Fuhrmann-Lieker, T.; Salbeck, J. *Chem. Rev.* **2007**, *107*, 1011.
13. Prelog, V.; Bedekovic, D. *Helv. Chim. Acta* **1979**, *62*, 2285.
14. Harada, N.; Ono, H.; Nishiwaki, T.; Uda, H. *J. Chem. Soc., Chem. Commun.* **1991**, 1753.
15. Alcazar, V.; Diederich, F. *Angew. Chem.* **1992**, *104*, 1503.
16. Cuntze, J.; Diederich, F. *Helv. Chim. Acta* **1997**, *80*, 897.
17. Jeon, S. O.; Jeon, Y. M.; Kim, J. W.; Lee, C. W.; Gong, M. S. *Org. Electron.* **2008**, *9*, 522.
18. Kim, K. S.; Jeon, Y. M.; Kim, J. W.; Lee, C. W.; Gong, M. S. *Org. Electron.* **2008**, *9*, 797.
19. Jeon, S. O.; Jeon, Y. M.; Kim, J. W.; Lee, C. W.; Gong, M. S. *Synth. Met.* In press.
20. Kim, K. S.; Jeon, Y. M.; Kim, J. W.; Lee, C. W.; Gong, M. S. *Synth. Met.* **2008**, *158*, 870.
21. Kim, K. S.; Jeon, Y. M.; Kim, J. W.; Lee, C. W.; Gong, M. S. *Dyes and Pigments* **2009**, *81*, 174.
22. Kim, J. H.; Jeon, Y. M.; Jang, J. G.; Ryu, S.; Chang, H. J.; Kim, J. W.; Lee, C. W.; Gong, M. S. *Bull. Korean Chem. Soc.* **2009**, *33*, 647.